



## Thermal conduction properties of microcracked media: Accounting for the unilateral effect

### *Propriétés de conduction thermique des milieux microfissurés : prise en compte de l'effet unilatéral*

Sharan Raj Rangasamy Mahendren, Hélène Weleman\* , Olivier Dalverny, Amèvi Tongne

Université de Toulouse, INP/ENIT, LGP, 47, avenue d'Azereix, 65016 Tarbes, France

#### ARTICLE INFO

##### Article history:

Received 10 April 2019

Accepted 7 October 2019

Available online 22 October 2019

##### Keywords:

Microcracking  
Heat conduction  
Thermal properties  
Homogenization  
Unilateral effect

##### Mots-clés :

Microfissuration  
Conduction thermique  
Propriétés thermiques  
Homogénéisation  
Effet unilatéral

#### ABSTRACT

Studies dedicated to the homogenization approach of microcracked media are largely focused on the determination of effective elastic properties. Some works investigate other properties, but most of them consider only open cracks. This paper intends to provide effective thermal properties related to the conduction problem taking into account the unilateral effect (opening/closure of cracks). Such analysis considers steady-state heat transfer within an initially isotropic media weakened by randomly oriented cracks. According to the boundary conditions, estimates and bounds based on Eshelby-like formalism are developed to derive closed-form expressions for effective thermal conductivity and resistivity in a fixed microcracking state.

© 2019 Académie des sciences. Published by Elsevier Masson SAS. This is an open access article under the CC BY-NC-ND license (<http://creativecommons.org/licenses/by-nc-nd/4.0/>).

#### R É S U M É

Les techniques d'homogénéisation des milieux microfissurés sont principalement employées pour l'étude des comportements mécaniques élastiques. D'autres applications sont également possibles, mais elles demeurent le plus souvent limitées à la considération de défauts ouverts. Ce travail vise à déterminer les propriétés effectives thermiques de milieux microfissurés dans le cadre d'une conduction stationnaire. Les matériaux étudiés sont initialement isotropes et présentent des microfissures d'orientation arbitraire pouvant être ouvertes ou bien fermées (effet unilatéral). S'appuyant sur une démarche de type Eshelby, les expressions des conductivités et résistivités effectives issues de différents schémas d'homogénéisation et bornes d'encadrement sont ici présentées et discutées.

© 2019 Académie des sciences. Published by Elsevier Masson SAS. This is an open access article under the CC BY-NC-ND license (<http://creativecommons.org/licenses/by-nc-nd/4.0/>).

\* Corresponding author.

E-mail address: [helene.weleman@enit.fr](mailto:helene.weleman@enit.fr) (H. Weleman).

### 1. Introduction

Homogenization is a useful tool for the modelling and analysis of the behaviour of heterogeneous materials. One of its main objectives is to estimate their overall properties from their microstructural features (phase properties, inclusions distribution and geometry, etc.). This topic is even more interesting when there is a lack of experimental data. Several studies have been dedicated to the micromechanical analysis of microcracked media, especially to address their elastic behaviour (for instance [1–3] for initially isotropic materials). Still, many practical applications require proper modelling of other properties such as thermal, transport and piezoelectric properties, which are not investigated much [4–8].

Taking into account the unilateral effect (opening and closure of cracks) makes the estimation of the said effective properties challenging, and this even more as microcracks are oriented defects. Some authors have investigated the elastic problem taking into account both the induced anisotropy and recovery phenomenon due to crack closure, through averaging up-scaling methods [1,9–11]. Such modelling strategy has never been applied before for a steady-state heat conduction problem. So, in this work, we intend to address this issue through an Eshelby-like approach and derive effective thermal properties of microcracked media, focusing mainly on the unilateral effect.

### 2. Theoretical framework

Assuming length scale separation, this study deals with continuum micromechanics. A homogenization process providing microstructure–properties relationships is conducted through mean-field theory. Present developments for effective thermal properties are inspired by the mathematical analogy between elasticity and steady-state heat conduction problems [12,13]:

$$\begin{aligned}
 \text{stress } \sigma &\iff \text{heat flux } q \\
 \text{strain } \epsilon &\iff \text{temperature gradient } g \\
 \text{stiffness } \mathbb{C} &\iff \text{thermal conductivity } \lambda \\
 \text{compliance } \mathbb{S} &\iff \text{thermal resistivity } \rho \\
 \text{Hooke's law} &\iff \text{Fourier's law}
 \end{aligned}$$

Similarly to the macroscopic stress and strain under equilibrium conditions, the macroscopic temperature gradient  $G$  (respectively macroscopic heat flux  $Q$ ) corresponds to the average values of its microscopic quantity  $g$  (resp.  $q$ ) under stationary thermal conditions [14]:

$$G = \frac{1}{\Omega} \int_{\Omega} g \, d\Omega = \langle g \rangle \quad \text{and} \quad Q = \langle q \rangle \tag{1}$$

with  $\Omega$  being the volume of the Representative Volume Element (RVE).

Moreover, the linear thermal behaviour is given by Fourier's heat conduction law:

$$q = -\lambda \cdot g \quad \text{and} \quad g = -\rho \cdot q \tag{2}$$

where  $\lambda$  (resp.  $\rho$ ) is the symmetric second-order thermal conductivity (resp. resistivity) tensor.

Let us consider a 3D RVE of a microcracked media. Such material exhibits a matrix-inclusion typology in which each phase (matrix, cracks) are supposed to exhibit a homogeneous behaviour. Two different boundary conditions can be imposed at the outer boundary  $\delta\Omega$  of the RVE, i.e. either uniform macroscopic temperature gradient ( $G$  imposed at  $\delta\Omega$ ) or uniform macroscopic heat flux ( $Q$  imposed at  $\delta\Omega$ ). Assuming an initial natural state, the microscopic and macroscopic quantities can be linked linearly as [15]:

$$g(x) = \mathbf{A}(x) \cdot G \quad \text{and} \quad q(x) = \mathbf{B}(x) \cdot Q \quad \forall x \in \Omega \tag{3}$$

where  $\mathbf{A}$  (resp.  $\mathbf{B}$ ) is the second-order gradient localization (resp. flux concentration) tensor such that  $\langle \mathbf{A} \rangle = \langle \mathbf{B} \rangle = \mathbf{I}$  ( $\mathbf{I}$  being the second-order identity tensor). The average temperature gradient  $G$  and heat flux  $Q$  of the heterogeneous media as obtained by (1) can thus be related by effective thermal tensors:

$$Q = -\lambda_{\text{hom}} \cdot G \quad \text{and} \quad G = -\rho_{\text{hom}} \cdot Q \tag{4}$$

where  $\lambda_{\text{hom}}$  (resp.  $\rho_{\text{hom}}$ ) is the overall thermal conductivity (resp. resistivity) of the microcracked media. Let denote  $\lambda_m$  and  $\rho_m = \lambda_m^{-1}$  the matrix conductivity and resistivity,  $\lambda_{c,i}$  and  $\rho_{c,i} = \lambda_{c,i}^{-1}$  the conductivity and resistivity of the  $i$ th ( $i = 1 \dots N$ ) family of parallel cracks and  $f_{c,i}$  their volume fraction. Simplifying assumptions regarding phase distribution allow approximating local fields within constituents by their phase averages, so that the overall thermal properties for the microcracked media can be given as:

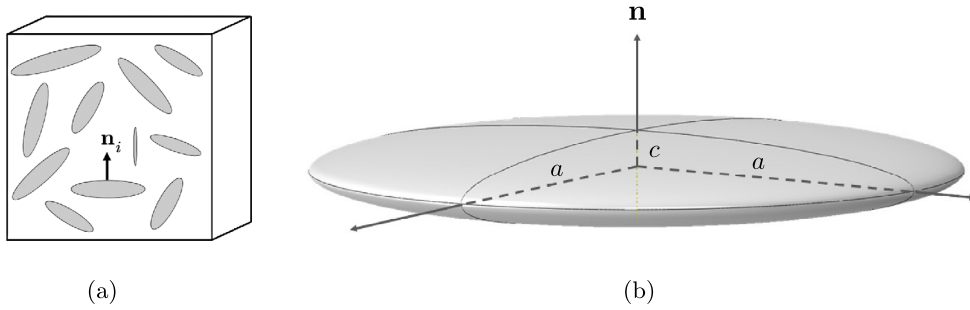


Fig. 1. (a) RVE with arbitrarily oriented microcracks, (b) penny-shaped crack geometry.

$$\lambda_{\text{hom}} = \lambda_m + \sum_{i=1}^N f_{c,i} (\lambda_{c,i} - \lambda_m) \cdot \langle \mathbf{A} \rangle_{c,i} \tag{5}$$

$$\rho_{\text{hom}} = \rho_m + \sum_{i=1}^N f_{c,i} (\rho_{c,i} - \rho_m) \cdot \langle \mathbf{B} \rangle_{c,i} \tag{6}$$

where  $\langle \cdot \rangle_r = \frac{1}{|\Omega_r|} \int_{\Omega_r} \cdot d\Omega$  denotes the average value over the volume of the phase  $r$  for  $r = \{m, c_i\}$ . At this point, effective tensors  $\lambda_{\text{hom}}$  (directly derived from uniform gradient-based boundary conditions) and  $\rho_{\text{hom}}$  (naturally obtained from uniform flux-based boundary conditions) strictly describe the same equivalent homogeneous media, so that these tensors are inverse of each other, i.e.  $\lambda_{\text{hom}} = \rho_{\text{hom}}^{-1}$ .

Following this modelling strategy, closed-form approximations of effective thermal tensors can be derived whenever localization and concentration tensors (denoted as  $\langle \mathbf{A} \rangle_{c,i}^{\text{est}}$  and  $\langle \mathbf{B} \rangle_{c,i}^{\text{est}}$  resp.) are estimated. Works on the single-inhomogeneity problem, initiated by Eshelby [16] in elasticity and extended to thermoelasticity [13,17], provide some solutions to such issue if the inclusions are ellipsoidal. Indeed, the temperature gradient and heat flux local fields in the crack can be approximated by the uniform respective local fields obtained in an ellipsoid embedded in an infinite matrix subjected to uniform boundary conditions denoted as  $G_\infty$  and  $Q_\infty$ . Assuming perfect interfaces, several representations can be developed according to the remote conditions, matrix properties, phase volume fractions, geometry and properties of the inhomogeneity.

For the present case, the RVE is composed of an initially isotropic homogeneous media, considered as the matrix. Its thermal conductivity and resistivity tensors are given by  $\lambda_m = \lambda_m \mathbf{I}$  and  $\rho_m = \rho_m \mathbf{I}$  ( $\lambda_m$  and  $\rho_m$  are the scalar thermal conductivity and resistivity, with  $\lambda_m = \rho_m^{-1}$ ) respectively. This matrix is weakened by randomly distributed microcracks with arbitrary orientations (Fig. 1a). A convenient way to represent such kind of defect is under the form of a flat oblate ellipsoid (mean semi-axes  $a$  and  $c$ , Fig. 1b). For the  $i$ th family of parallel microcracks,  $\mathbf{n}_i$  denotes their unit vector,  $\omega_i = c/a_i$  their mean aspect ratio, and  $d_i = \mathcal{N}_i a_i^2$  their scalar crack density parameter ( $\mathcal{N}_i$  is the number of cracks in the  $i$ th family per unit volume, [18]). The crack volume fraction is thus  $f_{c,i} = \frac{4}{3} \pi d_i \omega_i$ . Under these assumptions, estimated solutions for localization and concentration tensors  $\langle \mathbf{A} \rangle_{c,i}^{\text{est}}$  and  $\langle \mathbf{B} \rangle_{c,i}^{\text{est}}$  depend on the following depolarization tensor  $\mathbf{S}_i^E$  (similar to the Eshelby tensor of elastic problems) [19]:

$$\mathbf{S}_i^E = \left(1 - \frac{\pi}{2} \omega_i\right) \mathbf{n}_i \otimes \mathbf{n}_i + \frac{\pi}{4} \omega_i (\mathbf{I} - \mathbf{n}_i \otimes \mathbf{n}_i) \tag{7}$$

The last important points for the considered problem deal with the geometry and properties of the cracks. Regarding the former, the configuration of penny-shaped cracks corresponds to the limit case  $\omega_i \rightarrow 0$ , which must be introduced at the very end of the mathematical developments. Moreover, the fact that microcracks can be either open or closed according to compressive loads is introduced through the latter point. In both cases, cracks are assumed to be isotropic ( $\lambda_{c,i} = \lambda_{c,i} \mathbf{I}$  and  $\rho_{c,i} = \rho_{c,i} \mathbf{I}$ ), but they behave differently depending on the state of the microcrack:

- for the open case,  $\lambda_{c,i} = 0$  and  $\rho_{c,i} \rightarrow \infty$ , which corresponds to adiabatic conditions on the cracks lips,
- following the works of Deudé et al. [10], closed cracks are represented by a fictitious isotropic material with scalar conductivity  $\lambda_{c,i} = \lambda^*$  and resistivity  $\rho_{c,i} = \rho^*$ , which accounts for some heat transfer continuity at the closure of cracks (frictionless contact). Taking  $\lambda^* = \lambda_m$  and  $\rho^* = \rho_m$  may seem natural, but we will nevertheless continue the development for a general case where  $\lambda^*$  and  $\rho^*$  are scalars with the conditions  $\lambda^* \neq 0$  and  $\rho^* \neq \infty$ .

### 3. Gradient-based formulation

By gradient-based formulation, we mean to impose a uniform macroscopic temperature gradient  $G$  at the outer boundary  $\delta\Omega$  of the RVE. Such a situation corresponds to the classical strain-based condition of Eshelby’s problem. Let us consider three different approaches to derive the effective properties.

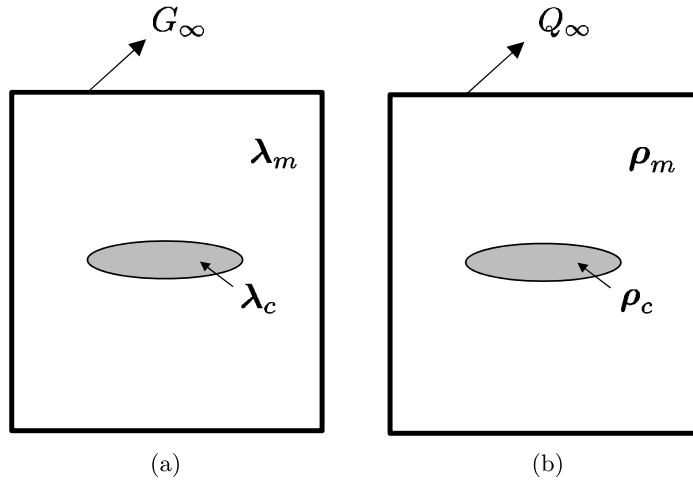


Fig. 2. Phase properties and boundary conditions at infinity: (a) imposed temperature gradient  $G_\infty$ , (b) imposed heat flux  $Q_\infty$ .

### 3.1. Dilute scheme

In a first approach, we are going to estimate the homogenized properties assuming a dilute density of cracks, which amounts to consider no interaction between defects. Remote conditions on the Eshelby problem lead in that case to the macroscopic gradient ( $G_\infty = G$ , see Fig. 2a). Hence, the gradient localization tensor is given by:

$$\langle \mathbf{A} \rangle_{c,i}^{\text{dil}} = \left[ \mathbf{I} + \mathbf{P}_i^E \cdot (\lambda_{c,i} - \lambda_m) \right]^{-1} \tag{8}$$

where  $\mathbf{P}_i^E = \mathbf{S}_i^E \cdot \rho_m$  is the symmetric second-order interaction tensor (equivalent to the first Hill tensor in elasticity). Eq. (8) can be simplified as:

$$\langle \mathbf{A} \rangle_{c,i}^{\text{dil}} = \left[ \mathbf{I} - \mathbf{S}_i^E (1 - \xi_i) \right]^{-1} \quad \text{with} \quad \xi_i = \frac{\lambda_{c,i}}{\lambda_m} \tag{9}$$

Eq. (5) thus leads to:

$$\lambda_{\text{hom}}^{\text{dil}} = \lambda_m \left[ \mathbf{I} - \frac{4}{3} \pi \sum_{i=1}^N d_i \omega_i (1 - \xi_i) \langle \mathbf{A} \rangle_{c,i}^{\text{dil}} \right] \tag{10}$$

We can see that the  $\lambda_{\text{hom}}^{\text{dil}}$  depends on the aspect ratio  $\omega_i$  in our case. However, we show that the quantity  $\omega_i (1 - \xi_i) \langle \mathbf{A} \rangle_{c,i}^{\text{dil}}$  tends to a limit  $\mathbf{T}_i$  when  $\omega_i \rightarrow 0$ , so:

$$\lambda_{\text{hom}}^{\text{dil}} = \lambda_m \cdot \left[ \mathbf{I} - \frac{4}{3} \pi \sum_{i=1}^N d_i \mathbf{T}_i \right] \quad \text{with} \quad \mathbf{T}_i = \lim_{\omega_i \rightarrow 0} \omega_i (1 - \xi_i) \left[ \mathbf{I} - \mathbf{S}_{E,i} (1 - \xi_i) \right]^{-1} \tag{11}$$

Such expansion includes both crack configurations, i.e., for open cracks  $\lambda_{c,i} = 0$ , so  $\xi_i = 0$ , while for closed cracks  $\lambda_{c,i} = \lambda^* \neq 0$ , so  $\xi_i \neq 0$ . Taking this into account, tensor  $\mathbf{T}_i$  for the  $i$ th family of cracks is given by:

$$\mathbf{T}_i = \begin{cases} \frac{2}{\pi} \mathbf{n}_i \otimes \mathbf{n}_i, & \text{if cracks are open} \\ \mathbf{0}, & \text{if cracks are closed} \end{cases} \tag{12}$$

Accordingly, Eq. (11) can be simplified as:

$$\lambda_{\text{hom}}^{\text{dil}} = \lambda_m \cdot \left[ \mathbf{I} - \frac{8}{3} \sum_{i/\text{open}} d_i \mathbf{n}_i \otimes \mathbf{n}_i \right] \tag{13}$$

in which only open cracks contribute in an additive manner. As an example, the effective thermal conductivity of a media weakened by a single family of parallel microcracks with unit normal  $\mathbf{n}$  and density  $d$  takes the form:

$$\lambda_{\text{hom}}^{\text{dil}} = \begin{cases} \lambda_m - \frac{8}{3} d \lambda_m \mathbf{n} \otimes \mathbf{n}, & \text{if cracks are open} \\ \lambda_m, & \text{if cracks are closed} \end{cases} \tag{14}$$

### 3.2. Mori–Tanaka scheme

In line with the Eshelby-like approach, the Mori–Tanaka (MT) scheme [20] considers cracks embedded in an infinite media (with matrix properties) that is subjected to the average temperature gradient over the matrix phase ( $G_\infty = \langle g \rangle_m$ , see Fig. 2a). Introducing inhomogeneities inside a thermally-stressed matrix in this way amounts to account for some interactions between cracks. Averaging rule (1) leads to the following localization tensor:

$$\langle \mathbf{A} \rangle_{c,i}^{\text{MT}} = \langle \mathbf{A} \rangle_{c,i}^{\text{dil}} \cdot \left[ f_m \mathbf{I} + \sum_{j=1}^N f_{c,j} \langle \mathbf{A} \rangle_{c,j}^{\text{dil}} \right]^{-1} \quad (15)$$

Now Eq. (5) can be written as:

$$\lambda_{\text{hom}}^{\text{MT}} = \lambda_m \cdot \left[ \mathbf{I} + \frac{4}{3} \pi \sum_{i=1}^N d_i \mathbf{T}_i \right]^{-1} = \lambda_m \cdot \left[ \mathbf{I} + \frac{8}{3} \sum_{i/\text{open}} d_i \mathbf{n}_i \otimes \mathbf{n}_i \right]^{-1} \quad (16)$$

since  $\lim_{\omega_i \rightarrow 0} \omega_i \left[ \mathbf{I} - \mathbf{S}_{E,i} (1 - \xi_i) \right]^{-1} = \mathbf{T}_i$  also. Accordingly, the specific conduction behaviour for the simple case of a single family of parallel microcracks according to their status described is as follows:

$$\lambda_{\text{hom}}^{\text{MT}} = \begin{cases} \lambda_m - \frac{8}{3} d \lambda_m \frac{1}{1 + \frac{8d}{3}} \mathbf{n} \otimes \mathbf{n}, & \text{if cracks are open} \\ \lambda_m, & \text{if cracks are closed} \end{cases} \quad (17)$$

### 3.3. Ponte Castañeda–Willis upper bound

Based on the Hashin–Shtrikman bounds [21], Ponte Castañeda and Willis (PCW) derived explicit strain-based bounds for the effective stiffness of composite materials with ellipsoidal inclusions [3]. Their estimate corresponds to a rigorous upper bound for the class of cracked media in which the matrix is the stiffest phase. The PCW formulation separately accounts for the inclusion shape and spatial distribution, respectively, through fourth-order interaction  $\mathbb{P}_i^E$  and spatial crack distribution  $\mathbb{P}_c^d$  tensors. Using a similar approach for the thermal problem with a second-order spatial distribution tensor  $\mathbf{P}_c^d$ , the effective conductivity can be given by:

$$\lambda_{\text{hom}}^{\text{PCW}} = \lambda_m + \left( \mathbf{I} - \sum_{i=1}^N f_{c,i} \left[ (\lambda_{c,i} - \lambda_m)^{-1} + \mathbf{P}_i^E \right]^{-1} \cdot \mathbf{P}_c^d \right)^{-1} \cdot \left( \sum_{i=1}^N f_{c,i} \left[ (\lambda_{c,i} - \lambda_m)^{-1} + \mathbf{P}_i^E \right]^{-1} \right) \quad (18)$$

It is also convenient to observe that:

$$\lambda_{\text{hom}}^{\text{PCW}} = \lambda_m \cdot \left( \mathbf{I} + \sum_{i=1}^N f_{c,i} \mathbf{M}_{c,i} \cdot \lambda_m \cdot \mathbf{P}_c^d \cdot \lambda_m \right)^{-1} \cdot \left( \mathbf{I} - \sum_{i=1}^N f_{c,i} \mathbf{M}_{c,i} \cdot \mathbf{Q}_c^d \right) \quad (19)$$

where  $\mathbf{M}_{c,i} = \left[ (\rho_{c,i} - \rho_m)^{-1} + \mathbf{Q}_i^E \right]^{-1}$ ,  $\mathbf{Q}_i^E = \lambda_m \cdot (\mathbf{I} - \mathbf{P}_i^E \cdot \lambda_m)$  (equivalent to the second Hill tensor in elasticity) and  $\mathbf{Q}_c^d = \lambda_m \cdot (\mathbf{I} - \mathbf{P}_c^d \cdot \lambda_m)$ . For simplicity, a spherical spatial distribution is adopted in this study, for which  $\mathbf{P}_c^d$  reads:

$$\mathbf{P}_c^d = \frac{1}{3} \rho_m \quad (20)$$

Even though, the PCW formulation is derived from the energy approach, Eq. (18) can be interpreted in the form of Eq. (5) through the following localization tensor:

$$\langle \mathbf{A} \rangle_{c,i}^{\text{PCW}} = \langle \mathbf{A} \rangle_{c,i}^{\text{dil}} \cdot \left( f_m \mathbf{I} + \sum_{j=1}^N f_{c,j} \left[ \mathbf{I} + (\mathbf{P}_j^E - \mathbf{P}_c^d) \cdot (\lambda_{c,j} - \lambda_m) \right] \cdot \langle \mathbf{A} \rangle_{c,j}^{\text{dil}} \right)^{-1} \quad (21)$$

As already emphasized by Ponte Castañeda and Willis, it can be observed that, when  $\mathbf{P}_c^d = \mathbf{P}_i^E$ , the PCW scheme corresponds to the Mori–Tanaka estimate (Eq. (21) comes to Eq. (15)) while the case  $\mathbf{P}_c^d = \mathbf{0}$  leads to the dilute approximation (Eq. (21) reduces to Eq. (8)).

Taking into account Eqs. (18)–(19), or equivalently Eqs. (21) and (5), the corresponding effective conductivity reads:

$$\lambda_{\text{hom}}^{\text{PCW}} = \lambda_m \cdot \left[ \mathbf{I} - \left( \frac{4}{3} \pi \sum_{i=1}^N d_i \mathbf{T}_i \right) \cdot \left( \mathbf{I} + \frac{4}{9} \pi \sum_{i=1}^N d_i \mathbf{T}_i \right)^{-1} \right] \quad (22)$$

Keeping in mind Eq. (12), one gets:

$$\lambda_{\text{hom}}^{\text{PCW}} = \lambda_m \cdot \left[ \mathbf{I} - \left( \frac{8}{3} \sum_{i/\text{open}} d_i \mathbf{n}_i \otimes \mathbf{n}_i \right) \cdot \left( \mathbf{I} + \frac{8}{9} \sum_{i/\text{open}} d_i \mathbf{n}_i \otimes \mathbf{n}_i \right)^{-1} \right] \tag{23}$$

which reduces to:

$$\lambda_{\text{hom}}^{\text{PCW}} = \begin{cases} \lambda_m - \frac{8}{3} d \lambda_m \frac{1}{1 + \frac{8d}{9}} \mathbf{n} \otimes \mathbf{n}, & \text{if cracks are open} \\ \lambda_m, & \text{if cracks are closed} \end{cases} \tag{24}$$

for a single family of parallel microcracks. Note that MT (Eq. (17)) and PCW (Eq. (24)) tend to dilute prediction (Eq. (14)) when  $d \rightarrow 0$ .

#### 4. Flux-based formulation

This section considers a uniform macroscopic heat flux  $Q$  at  $\delta\Omega$ . Estimates and bound are based on the local fields of cracks embedded inside a matrix subjected to a uniform heat flux at infinity ( $Q_\infty$ ). Accordingly, the temperature gradient  $g(x)$  tends to  $\rho_m \cdot Q_\infty$  when  $|x| \rightarrow \infty$ . This, therefore, amounts to the gradient boundary conditions of the Eshelby-like problem that provide the average temperature gradient  $\langle g \rangle_c$  over the cracks volume. From the average heat flux in this phase  $\langle q \rangle_c = \lambda_c \cdot \langle g \rangle_c$ , estimates of tensor  $\mathbf{B}$  can be derived.

##### 4.1. Dilute scheme

For the dilute scheme, the conditions at infinity correspond to the macroscopic heat flux ( $Q_\infty = Q$ , see Fig. 2b), so that

$$\langle \mathbf{B} \rangle_{c,i}^{\text{dil}} = \lambda_{c,i} \cdot \langle \mathbf{A} \rangle_{c,i}^{\text{dil}} \cdot \rho_m = \left[ \mathbf{I} + \mathbf{Q}_i^E \cdot (\rho_{c,i} - \rho_m) \right]^{-1} \tag{25}$$

Substituting Eq. (25) into Eq. (6), we get:

$$\rho_{\text{hom}}^{\text{dil}} = \rho_m \cdot \left[ \mathbf{I} + \frac{4}{3} \pi \sum_{i=1}^N d_i \mathbf{T}_i \right] \tag{26}$$

As previously mentioned, Eq. (26) accounts for the cracks state. For open cracks,  $\rho_{c,i} \rightarrow \infty$ , so again  $\xi_i = 0$ , while for closed cracks  $\rho_{c,i} = \rho^* \neq \infty$ , so  $\xi_i \neq 0$  with the related expression of the  $\mathbf{T}_i$  tensors provided in Eq. (12). Now,

$$\rho_{\text{hom}}^{\text{dil}} = \rho_m \cdot \left[ \mathbf{I} + \frac{8}{3} \sum_{i/\text{open}} d_i \mathbf{n}_i \otimes \mathbf{n}_i \right] \tag{27}$$

Taking this into account, the expression of the effective resistivity tensor for a single family of cracks becomes:

$$\rho_{\text{hom}}^{\text{dil}} = \begin{cases} \rho_m + \frac{8}{3} d \rho_m \mathbf{n} \otimes \mathbf{n}, & \text{if cracks are open} \\ \rho_m, & \text{if cracks are closed} \end{cases} \tag{28}$$

It should be noted that, according to the boundary condition, the dilute approximation leads to a different representation of the thermal behaviour in the open state of the cracks,  $\lambda_{\text{hom}}^{\text{dil}} \neq (\rho_{\text{hom}}^{\text{dil}})^{-1}$ . A similar result is obtained in elasticity as well. Yet, the effective conductivity and resistivity are obviously inverse of each other for the closed state of cracks,  $\lambda_{\text{hom}}^{\text{dil}} = (\rho_{\text{hom}}^{\text{dil}})^{-1}$ , while in this case strain-based or stress-based formulations of elasticity still remain different [11,22].

##### 4.2. Mori–Tanaka scheme

In this case, the remote conditions correspond to the average heat flux over the matrix phase ( $Q_\infty = \langle q \rangle_m$ , Fig. 2-b) and again, using the average rule, the flux concentration tensor is given by:

$$\langle \mathbf{B} \rangle_{c,i}^{\text{MT}} = \langle \mathbf{B} \rangle_{c,i}^{\text{dil}} \cdot \left[ f_m \mathbf{I} + \sum_{j=1}^N f_{c,j} \langle \mathbf{B} \rangle_{c,j}^{\text{dil}} \right]^{-1} \tag{29}$$

Introducing Eq. (29) into Eq. (6) finally gives:

$$\rho_{\text{hom}}^{\text{MT}} = \rho_{\text{hom}}^{\text{dil}} \tag{30}$$

From Eqs. (16), (27) and (30), it is clear that the Mori–Tanaka approach leads to the same predictions under gradient or flux conditions, both for open and closed microcracks, i.e.  $\lambda_{\text{hom}}^{\text{MT}} = (\rho_{\text{hom}}^{\text{MT}})^{-1}$ . The same conclusion has been drawn for elastic properties too [11,22].

### 4.3. Ponte Castañeda–Willis lower bound

As inspired by [3], Dormieux and Kondo [11] derived a variational stress-based lower bound for the effective compliance using an energy approach. Similarly to this work, the thermal resistivity can thus be given as:

$$\rho_{\text{hom}}^{\text{PCW}} = \left( \mathbf{I} - \sum_{i=1}^N f_{c,i} \mathbf{M}_{c,i} \cdot \mathbf{Q}_c^{\text{d}} \right)^{-1} \cdot \left( \mathbf{I} + \sum_{i=1}^N f_{c,i} \mathbf{M}_{c,i} \cdot \lambda_m \cdot \mathbf{P}_c^{\text{d}} \cdot \lambda_m \right) \cdot \rho_m \tag{31}$$

From Eqs. (19) and (31), we can observe the equivalence between the upper and lower PCW bounds, since  $\lambda_{\text{hom}}^{\text{PCW}} = (\rho_{\text{hom}}^{\text{PCW}})^{-1}$ . As for the gradient-based bound, the above estimate can be interpreted through the following concentration tensor:

$$\langle \mathbf{B} \rangle_{c,i}^{\text{PCW}} = \langle \mathbf{B} \rangle_{c,i}^{\text{dil}} \cdot \left( f_m \mathbf{I} + \sum_{j=1}^N f_{c,j} \left[ \mathbf{I} + (\mathbf{Q}_j^{\text{E}} - \mathbf{Q}_c^{\text{d}}) \cdot (\rho_{c,j} - \rho_m) \right] \cdot \langle \mathbf{B} \rangle_{c,j}^{\text{dil}} \right)^{-1} \tag{32}$$

Taking into account the spatial distribution adopted in Eq. (20), the flux-based PCW bound leads to the following effective thermal resistivity:

$$\rho_{\text{hom}}^{\text{PCW}} = \left[ \mathbf{I} + \left( \frac{4}{3} \pi \sum_{i=1}^N d_i \mathbf{T}_i \right) \cdot \left( \mathbf{I} - \frac{8}{9} \pi \sum_{i=1}^N d_i \mathbf{T}_i \right)^{-1} \right] \cdot \rho_m \tag{33}$$

After introducing Eq. (12), we get:

$$\rho_{\text{hom}}^{\text{PCW}} = \left[ \mathbf{I} + \left( \frac{8}{3} \sum_{i/\text{open}} d_i \mathbf{n}_i \otimes \mathbf{n}_i \right) \cdot \left( \mathbf{I} - \frac{16}{9} \sum_{i/\text{open}} d_i \mathbf{n}_i \otimes \mathbf{n}_i \right)^{-1} \right] \cdot \rho_m \tag{34}$$

For a single family example considered throughout the study, the above equation comes to:

$$\rho_{\text{hom}}^{\text{PCW}} = \begin{cases} \rho_m + \frac{8}{3} d \rho_m \frac{1}{1 - \frac{16d}{9}} \mathbf{n} \otimes \mathbf{n}, & \text{if cracks are open} \\ \rho_m, & \text{if cracks are closed} \end{cases} \tag{35}$$

which again tends to the dilute case (Eq. (28)) for  $d \rightarrow 0$ .

## 5. Discussion

We propose to highlight the consequences of microcracks on thermal properties through the case of a matrix with a single family of parallel cracks, for which closed-form expressions of dilute and Mori–Tanaka estimates and variational bounds have been provided in the text.

For the open cracks, we note that the material exhibits a damage-induced anisotropy, irrespective of the scheme or boundary conditions. To be precise, the effective thermal properties are transversely isotropic around axis  $\mathbf{n}$  of cracks (see Eqs. (14), (17), (24) and (28), (30), (35)). Especially, conductivity (respectively resistivity) is mostly degraded (resp. enhanced) along the direction orthogonal to the surface of the cracks, which is consistent with the adiabatic conditions on the lips of the cracks. As an illustration, Fig. 3 presents the rose diagrams of the generalized scalar conductivity  $\lambda(\mathbf{v})$  and resistivity  $\rho(\mathbf{v})$  in the direction of the unit vector  $\mathbf{v}$  defined by:

$$\lambda(\mathbf{v}) = \mathbf{v} \cdot \lambda_{\text{hom}} \cdot \mathbf{v} \quad \text{and} \quad \rho(\mathbf{v}) = \mathbf{v} \cdot \rho_{\text{hom}} \cdot \mathbf{v} \tag{36}$$

On the contrary, we note that closed cracks do not contribute to the degradation or enhancement of thermal conduction properties. This result is true regardless of the scheme, boundary conditions, fictitious properties ( $\lambda^*$ ,  $\rho^*$ ) or considered direction  $\mathbf{v}$ . Indeed, in all cases, effective conductivity and resistivity in any direction recover their initial value (of the virgin material) at the closure of microcracks, i.e.:

$$\lambda(\mathbf{v}) = \lambda_m \quad \text{and} \quad \rho(\mathbf{v}) = \rho_m, \quad \forall \mathbf{v}, \text{ if cracks are closed} \tag{37}$$

This means that the continuity of heat transfer is fully ensured when microcracks are closed, with a conduction response equal to that inside the homogeneous isotropic (virgin) matrix. Such a conclusion clearly differs from the results micromechanically established for elastic properties. Indeed, under frictionless conditions, crack closure leads to partial recovery of

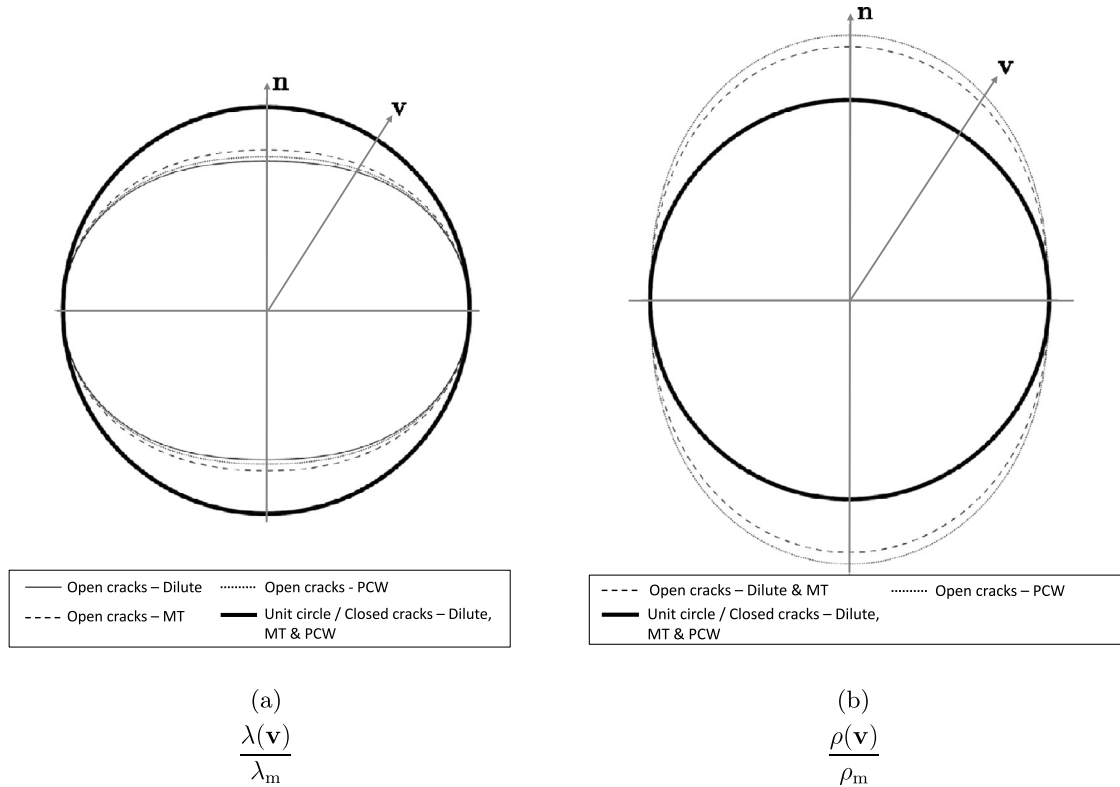


**Fig. 3.** Generalized thermal conductivity  $\lambda(\mathbf{v})$  and resistivity  $\rho(\mathbf{v})$  normalized by their initial values for a material weakened by a single family of parallel microcracks of unit normal  $\mathbf{n}$  (cracks density  $d = 0.1$ ).

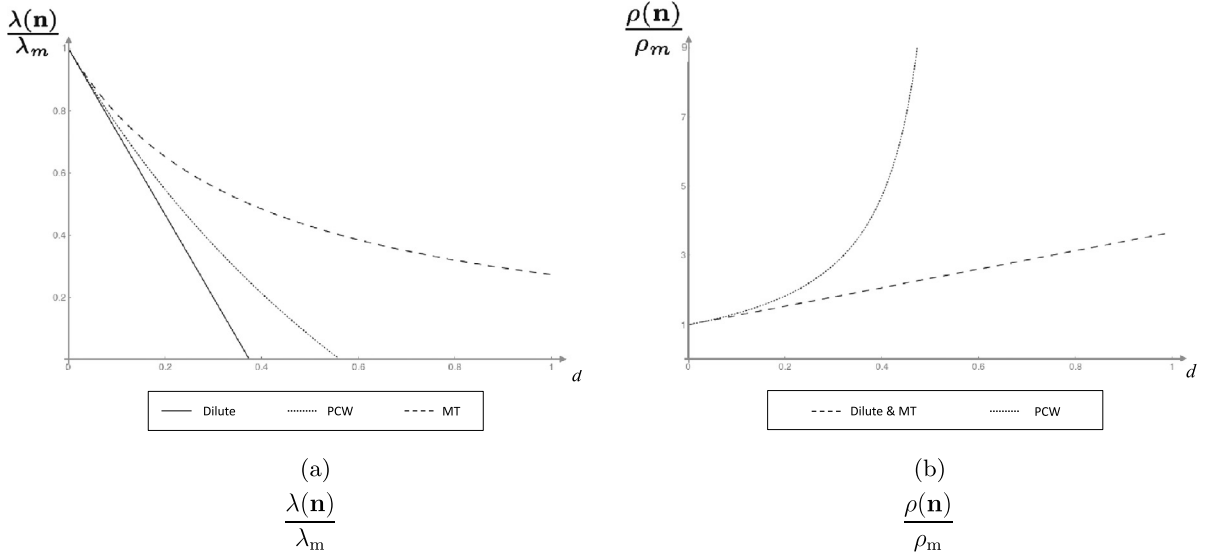


**Fig. 4.** Predictions of homogenization estimates and bounds for the generalized thermal conductivity  $\lambda(\mathbf{n})$  and resistivity  $\rho(\mathbf{n})$  for a material weakened by a single family of open parallel microcracks of unit normal  $\mathbf{n}$ .

mechanical properties. Considering, for instance, the Young modulus  $E(\mathbf{v}) = [\mathbf{v} \otimes \mathbf{v} : \mathbb{S} : \mathbf{v} \otimes \mathbf{v}]^{-1}$  (resp. the elongation modulus  $L(\mathbf{v}) = [\mathbf{v} \otimes \mathbf{v} : \mathbb{C} : \mathbf{v} \otimes \mathbf{v}]$ ) with  $\mathbb{S}$  the compliance tensor (resp.  $\mathbb{C}$  the stiffness tensor) for a stress-based formulation (resp. for a strain-based formulation), it has been demonstrated that closed cracks do not influence the Young modulus  $E(\mathbf{n})$  (resp. the elongation modulus  $L(\mathbf{n})$ ) in the direction  $\mathbf{n}$  normal to the cracks, but still remain active for others directions [23,24]. The complete damage deactivation for heat-conduction properties can be attributed to the lesser complexity of the problem itself and also to the simple definition of the depolarization tensor. Compared to elastic case, the Eshelby-like tensor  $\mathbf{S}^E$  for

conduction behaviour (Eq. (7)) contains only basic information, as it is of the second order, symmetric, and depends only on the aspect ratio  $\omega$  and the orientation  $\mathbf{n}$  of the crack (no dependency on the matrix properties, like the Eshelby tensor does in the elastic case for instance).

At last, it seems relevant to compare the homogenization estimates according to the microcrack density parameter. Conclusions for the closed state of microcracks are obvious since in all cases thermal properties are not affected by the defects. On the other hand, the open state shows some significant differences between dilute and Mori–Tanaka estimates and PCW variational bounds of conductivity, especially as crack density increases (Fig. 4(a)). Yet, similarly to compliance in elasticity, the Mori–Tanaka formulation coincides with the dilute case for resistivity (Eq. (30)). This is due to the combination of both the spatial crack distribution considered by MT (corresponding to Eshelby distribution) and the specific thermal resistivity of the open crack ( $\rho_c \rightarrow \infty$ ). Such point is confirmed by the evolution of the lower bound established in [11], which clearly differs from both previous schemes. Fig. 4(b) illustrates the significant role of interactions in resistivity prediction.

## 6. Conclusion

This note provides homogenization-based estimates and bounds of steady-state heat conduction properties for microcracked media. Especially, the influence of unilateral effects (according to the open or closed status of the cracks) on the effective thermal behaviour is taken into account. Results show that crack closure leads to a total recovery of the thermal conductivity and resistivity of the material, irrespective of the homogenization methods (taking into account or not interactions between microcracks) or boundary conditions. This thus provides relevant information for further works that will be dedicated to the thermo-mechanical modelling of materials with evolving damage.

## References

- [1] M. Kachanov, Elastic solids with many cracks and related problems, *Adv. Appl. Mech.* 30 (1993) 259–445.
- [2] S. Nemat-Nasser, M. Hori, *Micromechanics: Overall Properties of Heterogeneous Materials*, North-Holland Series in Applied Mathematics and Mechanics, vol. 37, Elsevier Science, Amsterdam, 1993.
- [3] P. Ponte Castañeda, J. Willis, The effect of spatial distribution on the effective behavior of composite materials and cracked media, *J. Mech. Phys. Solids* 43 (1995) 1919–1951.
- [4] L. Dormieux, D. Kondo, F.-J. Ulm, *Microporomechanics*, Wiley & Sons, Chichester, UK, 2006.
- [5] I. Sevostianov, M. Kachanov, On the effective properties of polycrystals with intergranular cracks, *Int. J. Solids Struct.* 156–157 (2019) 243–250.
- [6] D. Su, M.H. Santare, G.A. Gazonas, An effective medium model for elastic waves in microcrack damaged media, *Eng. Fract. Mech.* 75 (2008) 4104–4116.
- [7] X.D. Wang, L.Y. Jiang, The effective electroelastic property of piezoelectric media with parallel dielectric cracks, *Int. J. Solids Struct.* 40 (2003) 5287–5303.
- [8] A. Giraud, C. Gruescu, D.P. Do, F. Homand, D. Kondo, Effective thermal conductivity of transversely isotropic media with arbitrary oriented ellipsoidal inhomogeneities, *Int. J. Solids Struct.* 44 (2007) 2627–2647.
- [9] S. Andrieux, Y. Bamberger, J. Marigo, Un modèle de matériau microfissuré pour les bétons et les roches, *J. Méc. Théor. Appl.* 5 (1986) 471–513.
- [10] V. Deudé, L. Dormieux, D. Kondo, et al., Propriétés élastiques non linéaires d'un milieu mésofissuré, *C. R. Mecanique* 330 (2002) 587–592.
- [11] L. Dormieux, D. Kondo, Stress-based estimates and bounds of effective elastic properties: the case of cracked media with unilateral effects, *Comput. Mater. Sci.* 46 (2009) 173–179.
- [12] Z. Hashin, Analysis of composite material – a survey, *J. Appl. Mech.* 50 (1983) 481–505.
- [13] S. Torquato, *Random Heterogeneous Materials. Microstructure and Macroscopic Properties*, Springer Science+Business Media, New York, 2002.
- [14] B. Valès, V. Munoz, H. Welemane, et al., Heat source estimation in anisotropic materials, *Compos. Struct.* 136 (2016) 287–296.
- [15] R. Hill, Elastic properties of reinforced solids: some theoretical principles, *Int. J. Mech. Phys. Solids* 11 (1963) 357–372.
- [16] J.D. Eshelby, The determination of the elastic field of an ellipsoidal inclusion, and related problems, *Proc. R. Soc. A* 421 (1957) 379–396.
- [17] J.G. Berryman, Generalization of Eshelby's formula for a single ellipsoidal elastic inclusion to poroelasticity and thermoelasticity, *Phys. Rev. Lett.* 79 (1997) 1142–1145.
- [18] B. Budiansky, R.J. O'Connell, Elastic moduli of a cracked solid, *Int. J. Solids Struct.* 12 (1976) 81–97.
- [19] H. Hatta, M. Taya, Equivalent inclusion method for steady state heat conduction in composites, *Int. J. Eng. Sci.* 24 (1986) 1159–1172.
- [20] T. Mori, K. Tanaka, Average stress in matrix and average elastic energy of materials with misfitting inclusions, *Acta Metall.* 21 (1973) 571–574.
- [21] Z. Hashin, S. Shtrikman, A variational approach to the theory of elastic behavior of multiphase materials, *J. Mech. Phys. Solids* 11 (1963) 127–140.
- [22] Q.Z. Zhu, Applications des approches d'homogénéisation à la modélisation tridimensionnelle de l'endommagement des matériaux quasi fragiles: formulations, validations et implémentations numériques, PhD thesis, Lille, France, 2006.
- [23] H. Welemane, F. Cormery, Some remarks on the damage unilateral effect modelling for microcracked materials, *Int. J. Damage Mech.* 11 (2002) 65–86.
- [24] C. Goidescu, H. Welemane, D. Kondo, C. Gruescu, Microcracks closure effects in initially orthotropic materials, *Eur. J. Mech. A, Solids* 37 (2013) 172–184.